Investigation of the Nitrogen Hyperfine Structure of Vinylisocyanide by Microwave Fourier Transform Spectroscopy in the X- and Ku-Band

G. Bestmann and H. Dreizler
Abteilung Chemische Physik im Institut für Physikalische Chemie der Universität Kiel

Z. Naturforsch. **37a**, 58–63 (1982); received December 11, 1981

In memory of W. H. Flygare, University of Illinois, Urbana, USA

We discuss the features of a microwave Fourier transform spectrometer in the X- and Ku-band as applied to the investigation of the hyperfine structure of rotational transitions. The Nitrogen-hyperfine structure of vinylisocyanide was measured and analysed.

1. Introduction

Only very few investigations of isocyanide compounds [1–9] have been reported. The Nitrogen hyperfine structure (N-hfs) of methylisocyanide, CH_3-NC, was resolved [1]. As the isocyanides are unstable and reactive, it is interesting to know details about the electron distribution around the N-nucleus.

Following an investigation of vinylisocyanide, $CH_2=CH-NC$, of Yamada and Winnewisser [5], we measured and analysed the N-hfs of this molecule by use of a microwave Fourier transform spectrometer.

The construction of our microwave Fourier transform (MWFT) spectrometer in the Ku-band was reported in detail earlier [10]. Now we have extended our spectrometer to the X-band making some changes in the construction to obtain a higher sensitivity, resolution, and accuracy.

2. Experimental

A detailed diagram of the spectrometer is given in Figure 1. The signal source (1) is a phase stabilized (2 ... 8) microwave oscillator. The continuous microwave (mw) is pulse modulated (9 ... 12) with a pulse length ranging from 10 ns to 10 µs and a repetition rate of 3 kHz to 18 kHz.

The phase of the microwave pulse can be alternated (13 ... 16) by 180 degrees. This is done in a network with two pathes of equal length built with a SPDT pin diode switch, two equal waveguide twists and a power combiner. This network is nearly frequency independent. After amplification (17) the pulse reaches the sample cell (19 ... 22) with the molecular sample. The waveguide sample cell for the X-band has a length of 4 m. In the waveguide cell for the Ku-band of 12 m length we inserted two waveguide isolators mounted in vacuum tanks between three waveguide sections of equal length for minimizing reflections of the mw pulse (see [10]). So microwave windows within the cell are avoided. Both cells may be cooled to about 220 K.

The transient emission signal (for a detailed discussion see [11]) is preamplified by a low noise solid state mw amplifier (24) for improving the signal to noise ratio. The noise figures of the mw amplifiers are approximately 3 dB lower than those of the mixers (25). The pin diode switches (23, 18) protect the mw amplifier from the high power mw pulse and suppress the noise of the TWT amplifier (17) during the measurement period.

The emission signal is detected and converted downward to a center frequency of 160 MHz (25). This is done by a local oscillator (26) being phase stabilized 160 MHz above (or below) the signal oscillator (27 ... 35). After amplification and a second downward conversion (38, 39) with a local frequency of 130 MHz (33) the emission signal with a center frequency of 30 MHz is bandlimited from dc to 50 MHz (40).

It is also possible to convert the emission signal to dc (42, 43 and dashed lines) with a local frequency of 160 MHz. For the data acquisition we use a 1 bit transient recorder (44) with sample inter-

---

Reprint requests to Prof. Dr. H. Dreizler, Institut für Physikalische Chemie der Universität Kiel, Abt. Chemische Physik, Olshausenstraße 40–60, 2300 Kiel.

0340-4811 / 82 / 0100-0058 $ 01.00/0. — Please order a reprint rather than making your own copy.

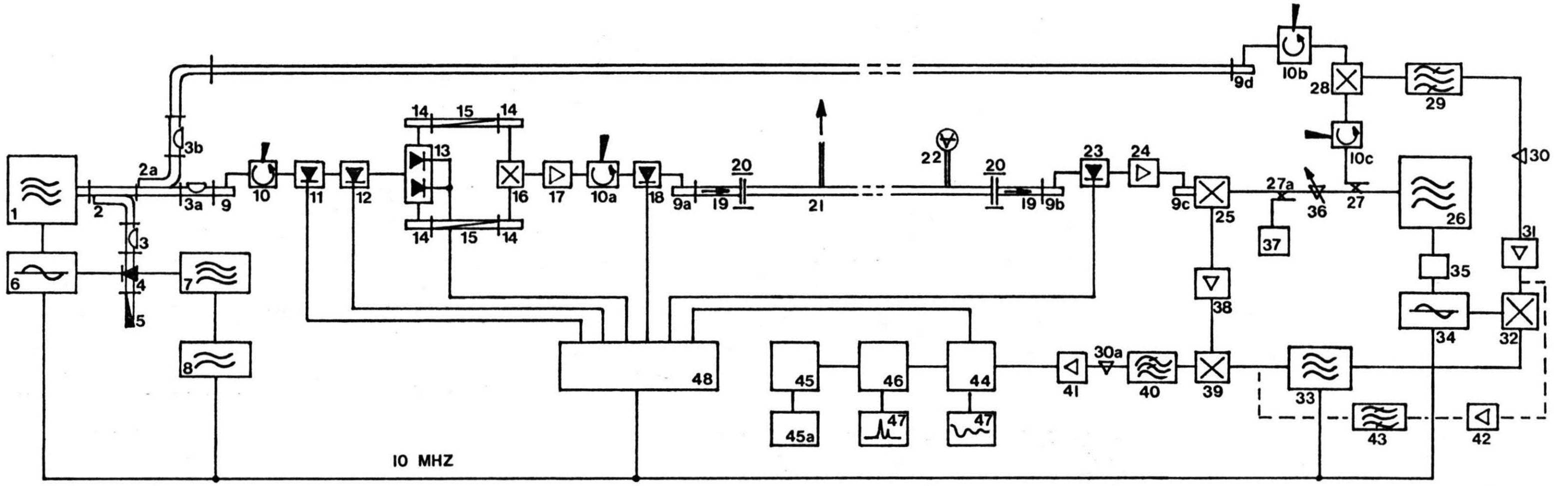

Fig. 1. Microwave Fouriertransform Spectrometer, X- and Ku-Band. List of devices and parts for the X-band, modifications for the Ku-band in parantheses, waveguides X- or Ku-band. 1. Backward wave oscillator, Hewlett Packard 8690B with 8694A (8695A); 2. Directional coupler, 10 dB; 3. Waveguide attenuator; 4. Waveguide mixer; 5. Termination; 6. Synchronizer, Rohde und Schwarz Type XKG; 7. Frequency standard, Rohde und Schwarz Type XUC; 8. Interpolation oscillator, Programmed Test Sources Type PTS160; 9. Waveguide to coax transition; 10. Isolator, coax; 11. PIN diode switch, Hewlett Packard 33144A with driver 33190B; 12. see 11.; 13. SPDT PIN diode switch, General Microwave Model F8928; 14. see 9.; 15. Waveguide twist 90 degrees; 16. Power divider, used as combiner, TRM DMS285-18; 17. TWT Amplifier Hughes 1177H03 (1177H04); 18. see 11.; 19. Waveguide isolator; 20. Microwave shielded cell window; 21. Sample cell and pump system, gas inlet; 22. Capacitance manometer, MKS Baratron 170M; 23. see 11.; 24. Microwave preamplifier, Miteq AIF-3A-1112-1 (Dexel DXA 5119-01); 25. Orthoguide double balanced mixer, RHG WMP 12C06EC (RHG WMP 12—18 BG54); 26. Backward wave oscillator (YIG tuned oscillator SDYX 3001, Systron Donner); 27. Directional coupler, coax; 28. MW mixer, Watkins Johnson M17C; 29. Bandpass filter 160 MHz; 30. Attenuator; 31. Amplifier 160 MHz; 32. IF mixer; 33. Frequency multiplier 10 to 130 MHz; 34. Synchronizer, Schomandl FDS30; 35. RC filter; 36. Attenuator, coax; 37. Microwave power meter; 38. see 31.; 39. see 32.; 40. Bandlimiting low pass filter; 41. Amplifier; 42. see 31.; 43. see 29.; 44. Transient recorder, 1024 × 1 bit, average system 1024 × 18 bit; 45. Mini computer TI 990/10 and terminal; 46. Output buffer; 47. Display unit; 48. Experiment control unit.

vals from 10 ns to 100 ns and up to 1024 data points in the time domain.

To improve the signal to noise ratio we average the transient emission signal in an 18-bit memory for up to 2^{18} cycles (44). After transferring the averaged data to a computer (45), we get the emission spectrum by calculating the power spectrum after a discrete Fourier transformation.

The time and frequency domain signals are shown on a display unit (47) and recorded on an XY-recorder.

3. Sensitivity

One limiting factor of the sensitivity of this type of spectrometer is the appearance of perturbing signals coherent to the system reference frequency.

A method of reducing these perturbations is to produce a mw pulse sequence with 180 degrees phase alternation. The transient emission signal changes its phase too. If the perturbations do not change their phase, an alternating addition and subtraction of the digitized transient emission signal increases the amplitude of the useful signal and decreases that of the perturbations. For an example of the success of this method see Fig. 2, in which we show a 50 MHz scan out of the rotational spectrum of $^{33}SO_2$ with and without suppression of coherent perturbing signals.

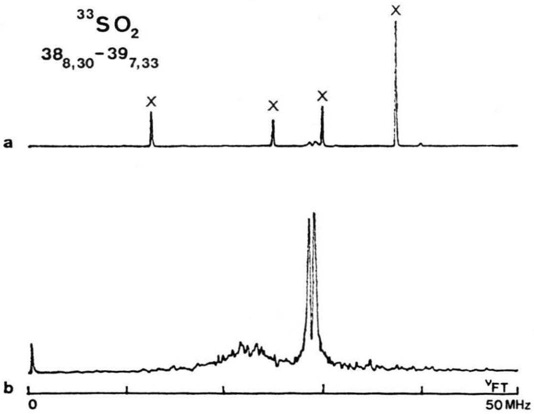

Fig. 2. Suppression of coherent perturbations (*) by a phase alternating pulse sequence; a) without and b) with suppression. The figure shows a 50 MHz scan out of the rotational spectrum of sulfurdioxide, SO_2, with $^{33}SO_2$ in natural abundance. Figure 2a is strongly expanded in the amplitude. Data acquisition: 1024 data points, 10 ns sample interval, 2^{18} averaging cycles, $p = 9$ mTorr, room temperature.

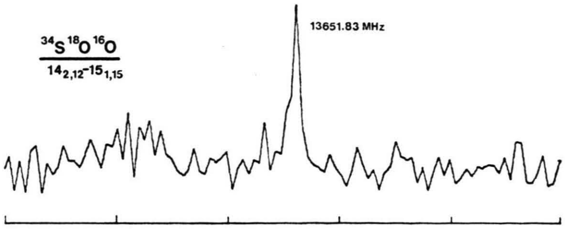

Fig. 3. A range of 10 MHz out of a 50 MHz scan of the rotational spectrum of sulfurdioxide, SO, with $^{34}S^{18}O^{16}O$ in natural abundance, Absorption coefficient $\alpha = 2.9 \times 10^{-10}$ cm^{-1} calculated from a value of [23] by the isotopic abundance. Data acquisition: 1024 data points, 10 ns sample interval, averaging in the time domain 2^{18} cycles, averaging in the frequency domain 16 cycles (total: 2^{22} cycles, 21 min), room temperature, $p = 10$ mTorr. (Frequency measured with enriched sample by [24]).

Another limiting factor of the sensitivity is a slow phase drift in the stabilization of the microwave oscillators. Signal averaging during a longer period than 30 minutes in the time domain does not increase the signal amplitude because the trigger signal phase of the transient recorder and the phase of the emission signal change. After a discrete Fourier transformation of the time domain signal the power spectrum is nearly independent of the phase of the transient emission signal. We average the emission signal for a maximum of 2^{18} cycles, transfer the collected data to the computer and automatically start a new averaging cycle. The data in the computer are Fourier-transformed and the power spectra of consecutive averaging cycles in the time domain are averaged in addition. So we are able to observe the improvement of the emission spectrum continuously.

The sensitivity of our present spectrometer is in the range of an absorption coefficient of 10^{-10} cm^{-1}. For an example see Fig. 3 which gives a range out of the rotational spectrum of $^{34}S^{18}O^{16}O$ in natural abundance (0.17×10^{-3}).

4. Resolution

The bandwidth of the spectrometer is given by the sampling theorem [12] to $\nu_B = 1/(2\,\Delta t)$. With a sample interval $\Delta t = 10$ ns we get a bandwidth of 50 MHz. After a Fourier transformation of the time domain signal the distance of the spectral points in the frequency domain is given by $\Delta\nu = 1/(N\,\Delta t)$. N is the number of sampled data points. With $N = 1024$ and $\Delta t = 10$ ns we get $\Delta\nu = 97.7$ kHz. Assuming a Lorentzian lineshape the resolution is approximately three times $\Delta\nu$. So we get a resolution of about 300 kHz.

For high resolution measurements we made some modifications in our data acquisition system. In such cases we measure with sample intervals of 20, 50 or 100 ns (bandwidth 25, 10 or 5 MHz) folding the transient emission signal from a range around 30 MHz into a range from 0 to 25, 10 or 5 MHz. For a 100 ns sample interval this for example gives a spectral point distance of 9.8 kHz and a resolution of about 30 kHz.

At the end of the measuring interval of 1024 data points we only average noise. So in experiments aiming at high resolution we may add zeroes up to 4096 data points prior to the Fourier transformation. The distance of the spectral points then becomes 2.4 kHz and we get a better interpolation of the frequency domain signal.

The IF mixing of the 160 MHz signal with the 130 MHz local frequency (33) may be replaced by mixing with 160 MHz derived from the output of (31). The low pass filter (40) should then be replaced by filters with lower cut off frequencies. With this arrangement we can measure without folding the transient emission signal. The results of both IF mixing procedures are comparable.

An example of a resolved multiplet pattern of the rotational transition $1_{0,1} - 0_{0,0}$ of vinylisocyanide is given in Figure 4. Figure 5 demonstrates the limit of the resolution so far obtained with our spectrometer.

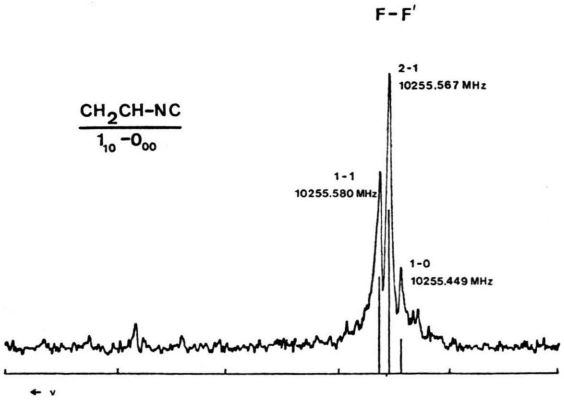

Fig. 4. Resolved multiplet scheme of vinylisocyanide $CH_2{=}CH{-}NC$. A range of 5 MHz out of a 10 MHz scan of the rotational spectrum. The lineshape is due to the power spectrum. Data acquisition: 1024 data points filled with zeroes up to 4096 data points, 50 ns sample interval, time domain averaging 2^{18} cycles, frequency domain averaging 4 cycles, $p = 0.3$ mTorr, $T = 223$ K.

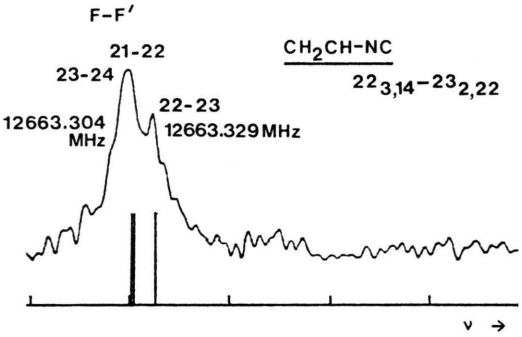

Fig. 5. Multiplet and theoretical multiplet scheme of vinylisocyanide. A range of 0.5 MHz out of a 5 MHz scan of the rotational spectrum. Data acquisition: 1024 data points filled with zeroes up to 4096 data points, 100 ns sample interval, time domain averaging 2^{18} cycles, frequency domain averaging 4 cycles, $p < 0.05$ mTorr, $T = 230$ K. (*Note added in proof:* $22_{3,19} - 23_{2,22}$.)

For high resolution measurements the pressure in the sample cell was less than 0.1 mTorr. For $CH_3C^{15}N$ a line width parameter of $\beta = 568$ kHz/mTorr was measured [13], which results in a linewidth at half height of $\Delta\nu = 18$ kHz for a pressure of 0.1 mTorr. In comparison to the linewidths in the spectra of other molecules, $CH_3C^{15}N$ seems to set an upper limit. For high resolution measurements wall and Doppler broadening now becomes a limiting factor for many molecules.

Besides the inherent advantages of MWFT spectroscopy – power and modulation broadening are absent – there is an additional advantage in comparison to Stark spectroscopy. Lines with sensitive Stark effect are broadened by not perfectly biased Stark square waves when using Stark spectroscopy. This fact was observed when investigating dimethylsulfoxide [14]. This is not the case for MWFT spectroscopy as no external field is present during the measurement of the transient emission.

5. Accuracy

The sample rate of the 1 bit transient recorder is synchronized with the 10 MHz system reference frequency. Thus the sample rate has the same accuracy as the reference. Assuming an uncertainty of 2 Hz we get for the emission signal frequency the uncertainty of the signal oscillator which is 2 kHz for a transition frequency of 10 GHz. The uncertainty in the spectral point distance $\Delta\nu$ is negligible.

The frequency of the Fourier-transformed transient emission signal is determined by a three point calculation assuming a Lorentzian lineshape. The

Table 1. Measured lines (ν_{exp}) of vinylisocyanide with N-hfs splittings. The intensity weighted mean frequency $\bar{\nu}$ is compared with measurements of [5], the hfs was calculated with χ^+ and χ^- from Table 2. Measuring accuracy 5 KHz, mean square deviation of the fit 3 KHz. All frequencies in MHz.

$J_{K_+K_-} - J'_{K_+'K_-'}$	$F - F'$	ν_{exp}	$\bar{\nu}$	ν [5]	$\Delta\nu_{\text{obs}}$	$\Delta\nu_{\text{cal}}$
$1_{0,1} - 0_{0,0}$	1 − 0	10 255.449	10 255.580	10 255.581	0.118	0.116
	2 − 1	10 255.567			0.077	0.077
	1 − 1	10 255.644				
$2_{1,2} - 3_{0,3}$	1 − 2	14 827.662	14 827.634	14 827.631	—	0.030
	3 − 4	14 827.662			0.087	0.085
	2 − 3	14 827.575				
$6_{1,5} - 6_{1,6}$	5 − 5	10 865.730	10 865.760	10 865.761	—	0.015
	7 − 7	10 865.730			0.092	0.090
	6 − 6	10 865.822				
$7_{1,6} - 7_{1,7}$	6 − 6	14 484.570	14 484.601	14 484.598	—	0.013
	8 − 8	14 484.570			0.095	0.091
	7 − 7	14 484.665				
$10_{2,9} - 11_{1,11}$	9 − 10	9 631.639	9 631.620	9 631.615	—	0.004
	11 − 12	9 631.639			0.056	0.053
	10 − 11	9 631.583				
$15_{2,13} - 15_{2,14}$	14 − 14	9 823.829	9 823.840	9 823.842	—	0.002
	16 − 16	9 823.829			0.034	0.029
	15 − 15	9 823.863				
$16_{2,14} - 16_{2,15}$	15 − 15	12 474.923	12 474.933	12 474.936	—	0.002
	17 − 17	12 474.923			0.031	0.032
	16 − 16	12 474.954				
$17_{2,15} - 17_{2,16}$	16 − 16	15 577.481	15 577.494	15 577.499	—	0.002
	18 − 18	15 577.481			0.040	0.035
	17 − 17	15 577.521				
$18_{2,16} - 19_{1,19}$	17 − 18	14 821.328	14 821.360	14 821.366	—	0.005
	19 − 20	14 821.328			0.095	0.086
	18 − 19	14 821.423				
$22_{3,19} - 23_{2,22}$	23 − 24	12 663.304	12 663.312	12 663.315	—	0.001
	21 − 22	12 663.304			0.025	0.022
	22 − 23	12 663.329				

uncertainty depends only on the actual lineshape and is up to 1 times the spectral point distance. The actual lineshape is given as a convolution of a Lorentzian lineshape with contributions from Doppler-broadening, wall collisions, noise and from overlapping multiplet lines.

The overall accuracy is the sum of the uncertainty of the signal oscillator and the uncertainty resulting from the calculation of the Fourier-transformed frequency.

6. Measurement

With the MWFT spectrometer in the X- and Ku-band (8 to 18 GHz) we measured the hyperfine structure of vinylisocyanide, $CH_2 = CH - NC$.

The substance was prepared by Jørn Johns. Christiansen. The measurements were made in the pressure region between 1 and 0.05 mTorr at 223 K. The measured lines are given in Table 1. The splittings were analyzed with first order theory [15] by fitting $\chi^+ = \chi_{bb} + \chi_{cc}$ and $\chi^- = \chi_{bb} - \chi_{cc}$. The rotational constants were taken from [5, Table 2]. 11 splittings were fitted with a mean square deviation of 3 kHz. The mean splitting is 68 kHz, the correlation coefficient is −0.059. There is no detectable dependence on χ_{ab} for $J = 0$ to $J = 8$ in the frequency region of the X- and Ku-bands. As an example two measured lines of vinylisocyanide are shown in Figures 4 and 5.

Table 2. Nitrogen coupling constants [MHz] of vinylisocyanide.

$\chi^+ = -0.258 \pm 0.005$; $\chi^- = -0.259 \pm 0.006$;
$\chi_{aa} = 0.258 \pm 0.005$; $\chi_{bb} = -0.258 \pm 0.006$;
$\chi_{cc} = -0.000 \pm 0.006$.

In summarizing our experiences in all our investigations we may state that microwave Fourier transform spectroscopy is at least complementary to microwave Stark spectroscopy.

We also measured in our laboratory the hyperfine structure of the following molecules: Benzonitrile, C_6H_5CN [16]; Nitrosobenzene, C_6H_5NO [17]; Deuterocyanoacetylene-^{15}N, $DCCC^{15}N$ [18]; cis-Allylcyanide $CH_3CHCHCN$ [19]; Butyronitrile, $CH_3CH_2CH_2CN$ [19]; and the internal rotation fine structure in the ground state of Dimethylsulfoxide, $(CH_3)_2SO$ [14]; Ethylfluoride, CH_3CH_2F [19]; Propionaldehyde, CH_3CH_2CHO [21]; trans n-Propanol, $CH_3CH_2CH_2OH$ [20]; Propionylfluoride, CH_3CH_2CFO [21]. In all cases the resolution could be improved in comparison to Stark spectroscopy. With the exemption of $(CH_3)_2SO$ [22] the fine structures were not observed by Stark spectroscopy earlier.

Acknowledgement

We thank Mr. Jørn Johns. Christiansen, Copenhagen, of the laboratory of Prof. Dr. M. Winnewisser, Giessen, for the preparation of the substance. Further we thank the members of our group for many discussions, the workshop of our institute for the craftmanship, the Deutsche Forschungsgemeinschaft and the Fonds der Chemischen Industrie for funds, Fa. Parzich und Co., Puergen, for the temporary loan of a TWT-amplifier.

[1] M. K. Kemp, J. M. Pochan, and W. H. Flygare, J. Phys. Chem. **71**, 765 (1967); CH_3-NC. — S. G. Kukolich, J. Chem. Phys. **57**, 4052 (1972); CH_3-NC with molecular beam.

[2] K. Bolton, N. L. Owen, and J. Sheridan, Spectrochim. Acta **25 A**, 1 (1969); CH_3-CH_2-NC.

[3] M. J. Fuller and E. B. Wilson jr., J. Mol. Spectr. **58**, 414 (1975); $CH_3CH_2CH_2$-NC.

[4] K. Bolton, N. L. Owen, and J. Sheridan, Spectrochim. Acta **26 A**, 909 (1970); $CH_2{=}CH{-}NC$.

[5] K. Yamada and M. Winnewisser, Z. Naturforsch. **30 a**, 672 (1975); $CH_2{=}CH{-}NC$.

[6] B. Bak, B. P. van Eijck, and C. Kierkegaard, J. Mol. Structure **18**, 429 (1973); C_6H_5-NC.

[7] B. Bak, L. Hansen-Nygaard, and J. Rastrup-Andersen, J. Mol. Spectr. **2**, 54 (1958); $(CH_3)_3C$-NC.

[8] R. R. Permanand and J. Sheridan, J. Mol. Struct. **70**, 297 (1981); C_3H_5-NC.

[9] R. A. Creswell, E. F. Pearson, M. Winnewisser, and G. Winnewisser, Z. Naturforsch. **31 a**, 221 (1976); H—NC.

[10] G. Bestmann, H. Dreizler, H. Mäder, and U. Andresen, Z. Naturforsch. **35 a**, 392 (1980).

[11] J. C. McGurk, T. G. Schmalz, and W. H. Flygare, Advances in Chemical Physics, Vol. 25, p. 1, J. Wiley, New York 1974.

[12] D. Ziessow, On-line Rechner in der Chemie, W. de Gruyter, Berlin 1973, p. 66.

[13] H. Mäder, H. Bomsdorf, and U. Andresen, Z. Naturforsch. **34 a**, 850 (1979).

[14] To be published.

[15] C. H. Townes and A. L. Schawlow, Microwave Spectroscopy, Chap. 6, McGraw Hill, New York 1955.

[16] E. Fliege, G. Bestmann, R. Schwarz, and H. Dreizler, Z. Naturforsch. **36 a**, 1124 (1981).

[17] E. Fliege, H. Dreizler, and U. Andresen, Z. Naturforsch. **36 a**, 1122 (1981).

[18] E. Fliege, G. Bestmann, M. Andolfatto, and H. Dreizler, Z. Naturforsch. **36 a**, 1126 (1981).

[19] To be published.

[20] H. Dreizler and F. Scappini, Z. Naturforsch. **36 a**, 1187 (1981).

[21] F. Scappini and H. Dreizler, Z. Naturforsch. to be published.

[22] H. Dreizler and G. Dendl, Z. Naturforsch. **20 a**, 1431 (1965).

[23] W. F. Kolbe, B. Leskovar, and H. Buscher, J. Mol. Spectr. **59**, 86 (1976).

[24] J. Bellet, C. Samson, and R. van Riet, Bull. Acad. Roy. Belg. **51**, 893 (1965).